INFLUENCE OF INDIVIDUAL INTERACTIONS ON HELICOPTER BLADE-VORTEX INTERACTION NOISE

Farhan Gandhi[1] and Lionel Tauszig[2]

Rotorcraft Center of Excellence
Department of Aerospace Engineering
The Pennsylvania State University
233 Hammond Building, University Park, PA 16802

Abstract

This paper describes a methodology to precisely evaluate the contributions of individual advancing and retreating side Blade-Vortex Interaction (BVI) events to the total radiated BVI noise, and demonstrates the results of its implementation. Such an analysis could be extremely useful in understanding which BVI events are acoustically dominant, and how BVI alleviation strategies work on weakening each of these dominant events. The methodology is based on first identifying the tip-vortex generating a particular interaction and then calculating the blade loading, acoustic pressure signal, and BVI sound pressure level due to this single vortex. This yields detailed quantitative information on – *(i)* the intensity and directionality of the noise due to individual events; and *(ii)* contribution of specific events to the total radiated BVI acoustic field. It is further demonstrated that the impulsive loads, acoustic pressure, and BVI noise can be predicted without loss of accuracy by considering only those portions of the tip vortices in close proximity of the blades in the 1st and 4th quadrants (instead of the entire tip vortices comprising the rotor wake).

1. Background

Parallel interactions between the helicopter main rotor blades and the strong tip vortices dominating the rotor wake result in impulsive blade loads that produce severe noise and vibration. Blade-Vortex Interaction (BVI) noise is a particularly serious problem in low speed and descending flight conditions when the tip vortices remain in close proximity of the rotor. Reducing approach noise is critical for community acceptance, which in turn is key for operation of helicopters and tilt-rotors from convenient city-center locations. On the military side, it is important to reduce the acoustic signature to avoid detection of helicopters approaching into hostile terrain. Reducing vibration associated with BVI would decrease crew, passenger, and structural component fatigue - for both military and civilian helicopters, and improve weapons accuracy of military helicopters. Consequently, significant effort has been devoted over the last several years to examining a variety of approaches for BVI alleviation. These approaches, which have included passive design concepts (such as advanced tip configurations, trailing edge spoilers, etc.), active control concepts (such as Higher Harmonic Control, Individual Blade Control, and Trailing Edge Flaps), and operational methods, have been very well summarized in a recent survey paper (Ref. 1). A host of similar research activities focusing on BVI alleviation are in progress at the present time.

A fair amount of previous and current research work focuses on analysis and understanding of the sources of BVI noise, and mechanisms by which noise reductions are obtained. However, this can be very complex because ***several distinct "parallel" or "near-parallel" blade-vortex interaction events contribute to the total BVI noise, making it very difficult to identify the individual contributions of these events***. For a 4-bladed rotor, 2-3 parallel BVI events on the advancing side and another 2 events on the retreating side are fairly typical. For a rotor with a larger number of blades (for example, the 5-bladed Comanche rotor), an even larger number of near-parallel BVI events could be expected on the advancing and retreating sides. While engineering intuition is often used to identify the most detrimental interactions, a precise numerical evaluation of the contribution of the individual events to the total BVI noise would be of considerable value. Such information could be exploited in developing focused strategies to weaken the strongest interactions and thereby reduce total BVI noise (while minimizing performance loss, power requirement in active strategies, etc.). Additionally, evaluating contributions

[1] Assistant Professor and corresponding author (e-mail: *fgandhi@psu.edu*, Tel: 814-865-1164, Fax: 814-865-7092)
[2] Graduate Research Assistant
Proceedings of the 26th European Rotorcraft Forum, Sept. 26-29, 2000, The Hague, The Netherlands

of individual interactions would enable us to ensure that a particular strategy, while weakening the strongest BVI events, did not strengthen or intensify some of the other interactions, or generate "new" interactions (thereby partially negating the benefits that would otherwise have been realized). Clearly, the value of a systematic and in-depth "diagnosis" of the contribution of the individual interactions to the total BVI noise cannot be over-emphasized.

2. Focus of the Present Study

The paper presents a novel methodology that can directly analyze the contributions of individual blade-vortex interaction events to the total BVI noise, and it seeks to highlight the usefulness of such an analysis. After determining the free-wake geometry, each advancing and retreating side BVI event (in the 1st and 4th quadrants of the rotor disk) is associated with a specific "generating" tip vortex released from a particular blade. *By considering the blade loading and acoustic pressure signal (at any observer location) due to individual tip vortices, the contribution of individual BVI events to the total BVI noise can be quantified*. The effectiveness and accuracy of this methodology is demonstrated through numerical simulation of blade loading, acoustic pressure histories, and BVI noise due to individual events, and comparisons with corresponding calculations for the entire wake. Further, the method is accelerated numerically by only considering portions of the tip vortices that produce near-parallel interactions with the blade in the 1st and 4th quadrant of the rotor disks, and it is demonstrated in the paper that the main characteristics of the impulsive blade loading and the radiated noise are captured very accurately using such an approach.

3. Approach

Evaluation of the blade-vortex interactions and the resulting noise requires, first and foremost, an accurate determination of the rotor wake, and the positions of the tip vortices relative to the blade. A free-wake formulation based on the Maryland Free Wake (MFW) algorithm [2] is used to calculate the geometry and strength of the tip vortices. The algorithm has been independently implemented at the Pennsylvania State University [3] and validated by comparing the predicted inflow, wake geometry, and BVI locations, to previously published results. This implementation is specifically focused toward numerically identifying occurrence of blade-vortex interactions [4, 5], and therefore uses a *system of overlapping low- and high-resolution azimuthal grids.* For computational efficiency, the free-wake geometry is explicitly evaluated only at 80 azimuthal stations over a rotor revolution (low-resolution grid). After computing the free-wake geometry (and the rotor blade response), a reference blade is allowed to time-march around the azimuth in very small increments; and BVIs are identified based on blade-vortex "miss-distance" (see Ref. 5) and/or impulsive changes in blade loading. A high-resolution azimuthal grid comprising of 640 azimuthal steps is used for this purpose, with the wake geometry at any point on this grid obtained by interpolating the geometry evaluated at the low-resolution grid points. Such interpolation of free-wake geometry onto high-resolution grids for BVI detection has been used by other researchers (for example, Refs. 6, 7). It is possible to associate individual advancing as well as retreating side *parallel BVI events* (which are the ones of interest) to specific "generating" tip vortices in the rotor wake, although this has not always been done in the literature.

The high-resolution airloads are then used as input to the rotorcraft acoustic code WOPWOP [8], which provides the acoustic pressure signal over a rotor revolution at any specified observer location. From the acoustic pressure signal, the BVI sound pressure level (BVISPL) is calculated by typically considering the 6th to the 40th harmonics of the blade passage frequency. The BVISPL is used as the metric for BVI noise. By computing the acoustic pressures and BVISPL at several observer locations on a plane below the rotor (or alternatively on a semi-sphere), information on both directivity as well as intensity of the total radiated BVI noise is obtained.

While a procedure such as described above is fairly typical in most studies examining BVI, it fails to clearly identify the specific contribution of individual BVI events to the total radiated noise field. Conversely, since the intensity and directivity of the noise associated with the various BVI events is not individually calculated, it is very difficult to conclusively identify the acoustically dominant BVI events (although educated guesses are possible). Consequently, strategies that specifically target weakening the most dominant events have not been aggressively pursued, nor is it possible to evaluate the effectiveness of commonly used BVI alleviation strategies, on the worst (as well as the milder) BVI events. Such an evaluation would be useful to ensure that a particular BVI alleviation scheme, while reducing the overall BVI noise, did not intensify certain interactions (thereby reducing the potential benefits that could be achieved).

The approach described below addresses this issue of identifying the contribution of individual BVI events on the total BVI noise. After calculating the free-wake geometry and identifying all the parallel or near-parallel BVI events (on the advancing and retreating sides - 1st and 4th quadrants), the generating tip vortex responsible for each BVI event must be identified. If the "miss-distance" method is used to detect occurrence of BVI, this information is already available (see Ref. 5). If impulsive change in blade loading is used to detect occurrence of BVI, snapshots

of the wake geometry when the blade is frozen at the azimuthal locations corresponding to the interactions can be used to identify the generating tip vortex. For the 4-bladed rotor considered in this study, the tip vortex released by the blade preceding the reference blade, k, is denoted as the (k-1) vortex, that released by the opposite blade is denoted as the (k-2) vortex, the vortex released by the next blade is (k-3), and that of the reference blade itself is referred to as the (k-0) vortex.

Once the generating tip vortex producing a particular BVI event has been identified, a detailed analysis of that individual event can be carried out by considering that vortex alone. For example, if it is determined that a particular BVI is produced by the (k-1) vortex, all the other vortices are "switched off" (by setting the circulation to zero or simply not considering them), and the inflow and loading due to the remaining (k-1) vortex is calculated as the reference blade marches around the azimuth (depicted schematically in Fig. 1). This blade loading is then used as input to the acoustic code WOPWOP, to calculate the acoustic signals and BVISPL on an observer plane. Clearly, the resulting BVISPL (intensity and directivity) can be attributed to the specific BVI event considered (and the tip vortex generating that event). This procedure is then repeated for each of the BVI events. A direct comparison of the BVISPL maps due to the various tip vortices (or BVI events) would immediately reveal the acoustically dominant interactions and provide detailed information with regard to their relative intensity and directionality. A comparison of BVISPL maps due to individual vortices to the BVISPL map due to the entire wake would provide interesting insight about how these individual events combine to produce the total radiated BVI noise that would be experienced by an observer.

Finally, recognizing that the BVI noise is dominated by the impulsive changes in blade loading associated with parallel interactions in the 1st and 4th quadrants, it is proposed (and verified in Section 5) that only the vortical segments in these quadrants that pass in close proximity of the rotor blade need to be considered (rather than considering entire tip vortices). Figure 6 schematically represents this concept. To evaluate the influence of an advancing side parallel BVI generated by the (k-1) vortex, only that portion of the (k-1) vortex passing in close proximity of the blade in the 1st quadrant is considered, with the rest of the (k-1) vortex "switched off" in addition to the other vortices. It is shown in Section 5 that the impulsive loading and BVI noise predicted using only these vortical segments compare well with corresponding results for an entire 4-revolution long tip vortex. It is also shown that by systematically considering all the segments that produce close parallel interactions in the 1st and 4th quadrants (from the various tip vortices), the total loading and BVI noise predictions are close to those obtained using the entire wake.

4. Advantages of Present Approach

The approach proposed in the previous section can evaluate, with precision, the contribution of various BVI events to the total radiated BVI noise - at a given observer location, or over an entire observer plane or semi-sphere (this is supported by results in Section 5). The only other method previously reported in the rotorcraft literature that associates recorded acoustic signals with noise sources is the *Acoustic Ray Tracing Technique* [9, 10]. This section highlights some of the unique features of the present approach and some advantages over the *Acoustic Ray Tracing Technique*, as a means to identify locations on the rotor disk where a blade-vortex interaction may have occurred. Primarily developed for experimental studies, the Acoustic Ray Tracing Technique considers the acoustic waveforms at a number of microphone (observer) locations with prominent and easily identifiable BVI impulses, and then uses geometric triangulation to identify possible source locations on the rotor disk. For each of these possibilities, the instant of BVI impulse emission is calculated, and the location of the blade at that instant is used to pinpoint the actual source location. The accuracy of the triangulation technique is strongly dependent on engineering judgement in interpreting acoustic time histories and identifying specific BVI occurrences. This can be particularly difficult when the acoustic signal has multiple impulses associated with different BVI events. Clearly, acoustic ray tracing represents an "inverse" technique (identifying source from acoustic pressure signal). In contrast, the approach presented in the paper is "direct" in that it starts with the source, the impulsive loading due to a BVI event, and proceeds to calculate the resultant noise due to this event. It should also be emphasized that the present approach associates an individual BVI event (and the corresponding acoustic pressure histories) with a generating vortex, and additionally provides the noise directivity due to this event. Even when Acoustic Ray Tracing accurately identifies the source location on the rotor disk, information with regard to the generating vortex is not directly available. Further, although source location on the rotor disk may be available through Ray Tracing, the directionality of the radiated noise from individual BVI events is not clearly identifiable.

5. Results and Discussion

Numerical simulations are conducted using a UH-60 model rotor previously tested at NASA Langley Research Center [10]. The rotor considered has a 2.856 meter diameter with a NACA 0012 airfoil, a 9.1 cm chord, a 10 deg. linear twist, and a 217.11 m/s tip speed. A 4.1 deg. backward shaft angle and an

advance ratio 0.14 are used in the simulations, representing a high-BVI condition. The rotor is in a wind-tunnel trim condition with a thrust coefficient of 0.007, and cyclic pitch controls to eliminate 1st harmonic blade flapping.

As a reference blade marches around the azimuth, it experiences several blade-vortex interactions on both the advancing and retreating sides. These interactions, detected using the "planar" or "miss-distance" method [5], are shown in Fig. 2 as bands on the rotor disk representing passage of tip vortices in proximity of the blades. The width of the band represents the miss-distance of the vortex from the blade (greater band width implying that the vortex is very close to the blade or passing through the blade). Further, a light grey shade is used to indicate that the interacting vortex is above the blade whereas the dark grey is used to indicate that the vortex is below the blade. On Fig. 2a a snapshot of the geometry of the tip vortices is superposed for the case when the reference blade is at ψ=285°. Similarly, Fig. 2b shows the geometry of the tip vortices when the reference blade is at ψ=60°. Superposing the tip-vortex geometry in such a manner facilitates identification of the source of the BVI for both advancing side interactions (Fig. 2b) as well as retreating side interactions (Fig. 2a); since interaction "bands" on both figures can now be associated with specific tip vortices. With the tip vortices from the different blades represented using different line styles, it can be deduced from Fig. 2b (reference blade, k, at ψ = 60°) that the advancing side BVI denoted as I is due to interaction with the vortex from the preceding blade, (k-1). Similarly, it can be seen that the BVI, II, is generated by the tip vortex from the opposite blade, (k-2), and the BVI, III, is due to interaction with the (k-3) tip vortex. The interactions with the (k-2) and (k-3) vortices (marked as II and III, respectively) are particularly parallel, and likely to produce significant impulsive noise. In a similar manner, it can be deduced from Fig. 2a (vortex geometry corresponding to reference blade, k, at ψ = 285°) that the retreating side BVI marked as V (around at ψ = 280°) is due to the (k-3) vortex, whereas the BVI marked as IV (around at ψ = 295°) is due to the (k-0) vortex (released by the reference blade itself).

Next, the high-resolution blade loads (based on the computed free-wake geometry) are calculated by allowing the reference blade to time-march around the azimuth in very small increments (640 steps used per revolution). This high-resolution blade loading is used as an input to the rotor acoustic code, WOPWOP [8], which yields the acoustic pressure signal, which is then used to obtain the BVISPL on an observer plane. Figure 3a shows the BVISPL on a 16x16 grid of points (observer locations) in a horizontal x-y plane 1.6m below the rotor (rotor radius is 1.428m). The contours represent lines of constant BVI sound pressure levels, with the darker shades denoting regions of higher BVI noise. A focused region of high BVI noise can be seen on the advancing side, and another focused region (of somewhat lower intensity) is directed toward the back of the disk due to the retreating side BVI. The general noise directivity shows good qualitative comparison with measurement, such as that from the HART test [11]. While this plot is valuable in that it gives the noise radiated by all the BVIs, it is difficult to extract from it the relative importance of the individual BVI events.

Figures 3b-3e, respectively, show the BVISPL (on the same observer plane) associated with *individual vortices* (k-0), (k-1), (k-2) and (k-3). In each case, the loading on the reference blade is calculated due to a *single vortex* (with all others "switched off'). For example, Fig. 3c is generated by calculating the loading due to the preceding (k-1) vortex only, *and using this as an input to WOPWOP*. Clearly, it is the (k-2) and (k-3) interactions (for this rotor and flight condition) that contribute strongly to the advancing side BVI noise (see Figs. 3d and 3e); with relatively insignificant contributions from the (k-0) and (k-1) vortices (see Figs. 3b and 3c). This observation is consistent with Fig. 2b, which shows strong parallel interactions with the vortices (k-2) and (k-3) on the advancing side. Similarly, it is clearly seen that the (k-0) interaction (Fig. 3b) and the (k-3) interaction (Fig. 3e) contribute to the BVI noise directed toward the back of the disk. This is again consistent with Fig. 2a, which shows somewhat parallel interactions with the vortices (k-0) and (k-3) on the retreating side. It is important to note that with the approach presented in this paper, ***quantitative estimates*** of the contributions of various interactions to the total advancing and retreating side BVI noise are available. It is also very interesting to note that the differences in directionality of the radiated noise due to the various BVI events (compare Figs. 3d and 3e, for example) could be attributed to differences in "event type" as categorized in a simple but fundamental study reported in Ref. 12.

At the advancing side observer location corresponding to peak total BVI noise (x = –0.2m, y = –1.5 m, see Fig. 3a), the acoustic pressure signals due to the individual vortices are shown in Figs. 4a-4d, while the acoustic pressure signal obtained by considering the entire wake is shown in Fig. 4e. Comparing Figs. 4a-4d, it is evident that the (k-2) and (k-3) interactions (Figs. 4c and 4d, respectively) produce the largest impulsive changes in acoustic pressure – responsible for high BVI noise intensity. In Fig. 4e the dashed line represents the acoustic pressure calculated by considering the blade loading due to the entire wake (referred to as "direct calculation"), whereas the solid line represents a superposition of the acoustic pressure signals of Figs. 4a-4d. The excellent agreement between the two calculations in Fig. 4e verifies that the decomposition approach presented, and used for examination of contributions of individual vortices, is

valid and accurate. Further, by comparing the total acoustic pressure signal due to the entire wake (Fig. 4e) to the signals due to individual vortices (Figs. 4a-4d), it is possible to link specific impulses in the total acoustic pressure signal to specific BVI events (interactions with specific vortices). For example, comparing Fig. 4e to Figs. 4a-4d, it is easy to conclude that the first impulsive change in the acoustic pressure signal in Fig. 4e is due to the (k-3) interaction (see Fig. 4d), whereas the second impulse is due to the (k-2) interaction (see Fig. 4c). Without the decomposition approach used, this type of identification would be very difficult.

The solid line in Fig. 4e, *obtained by adding the acoustic pressures due to individual vortices*, is used to calculate the BVISPL at the observer location (-0.2, -1.5). Next, this process of superposing the acoustic pressure signals due to individual vortices and calculating the resulting BVISPL is repeated at every observer location in the plane (results plotted in Fig. 5). Figure 5 shows excellent overall agreement with Fig. 3a (obtained by simply considering the entire wake), and provides additional confidence in the validity and accuracy of the procedure presented in this paper.

Next, the question of how accurately the BVI noise can be predicted considering only those portions of the vortices that produce close and nearly parallel interactions in the 1st and 4th quadrants (rather than the entire vortices) is addressed. Figure 6 shows a schematic of the reference blade and the tip vortex from the preceding (k-1) blade, with a portion producing an advancing side BVI (in the 1st quadrant) highlighted. Similarly, the segment of the (k-1) vortex that passes in proximity of the reference blade in the 4th quadrant, as well as segments of the (k-2), (k-3), and (k-0) vortices that produce close, near-parallel interactions with the blade in the 1st and 4th quadrants are considered. Since the (k-2) and (k-3) interactions on the advancing side have been found to be the most severe, detailed numerical simulations to demonstrate the viability of considering only portions of the vortex, will focus primarily on these interactions. Figures 7a and 7b, respectively, show the disk loading and loading as a function of azimuthal location at 80% radial location, obtained by considering the entire (k-2) vortex (solid lines) and the portion of the (k-2) vortex producing close, near-parallel interactions in the 1st and 4th quadrants (dashed lines). Clearly, the significant impulsive change in lift on the advancing side in Fig. 7a is adequately captured using only the vortical segments (good agreement between dashed and solid lines). While good agreement in any impulsive changes in lift in the 1st and 4th quadrants is intuitively expected, it should be noted that overall agreement over the entire disk is surprisingly good. Again, in Fig. 7b, the sharp impulsive change in loading in the 1st quadrant and a milder impulse in the 4th quadrant, captured using only the vortical segments compare well with the results obtained using the entire vortex. The comparison at other azimuthal locations generally appears satisfactory. Similarly, Figs. 8a and 8b, respectively, show the disk loading and loading at 80% radial location, obtained by considering the entire (k-3) vortex (solid lines) and the portions of the (k-3) vortex in close proximity of the blade in the 1st and 4th quadrants (dashed lines). As in Figs. 7, it is clear from Figs. 8a and 8b that the loading predicted using only the (k-3) vortical segments in proximity of the blade in the 1st and 4th quadrants compares well with the loading due to the entire vortex.

Figures 9a and 9b, respectively, show the disk loading and loading as a function of azimuthal location at 80% radial location, obtained by considering – *(i)* the entire wake, comprising of the entire (k-1), (k-2), (k-3) and (k-0) vortices (solid lines); and *(ii)* the segments of the (k-1), (k-2), (k-3) and (k-0) vortices in close proximity of the blade in the 1st and 4th quadrants (dashed lines). The blade loading calculated using only the vortical segments compares extremely well with that obtained for the entire wake (see both the disk plot, Fig. 9a, as well as the loading at 80% radial location, Fig. 9b).

Figure 10a shows the BVISPL on the observer plane below the rotor using only the loading due to the (k-2) vortical segments in proximity of the blade in the 1st and 4th quadrants. The predicted noise radiation (both intensity and directionality) show excellent agreement with that obtained using the entire (k-2) vortex (compare with Fig. 3d). Similarly, Fig. 10b shows the BVISPL using only the loading due to the (k-3) vortical segments in proximity of the blade in the 1st and 4th quadrants. Again, the predicted noise radiation (intensity and directionality) show excellent agreement with that obtained using the entire (k-3) vortex (compare with Fig. 3e). A detailed examination of the acoustic pressure signals at the observer location of maximum total BVI noise is presented in Fig. 11. Figure 11a shows the acoustic pressure history due to the 1st and 4th quadrant (k-2) vortical elements (dashed line), and this is seen to compare very well to the acoustic pressure calculated due to the entire (k-2) tip vortex (solid line). Similarly, in Fig. 11b the acoustic pressure history due to the 1st and 4th quadrant (k-3) vortical elements compares very well to the acoustic pressure calculated due to the entire (k-3) tip vortex.

From the results presented above it can be deduced that the impulsive changes in blade loads (Figs. 7-9), impulsive changes in acoustic pressure (Fig. 11), and the BVISPLs (Fig. 10) can be accurately predicted considering only the portions of the tip vortices in the 1st and 4th quadrant producing close, near-parallel interactions (rather than the entire free-wake geometry).

6. Concluding Remarks

This paper describes a methodology to quantitatively determine the contributions of individual advancing and retreating side Blade-Vortex Interaction (BVI) events to the total radiated BVI noise. After computing the free-wake geometry and identifying the blade-vortex interactions, the tip-vortices generating each of these events needs to be determined. Then, to evaluate the influence of a particular BVI event, the blade loading due to the "generating vortex" is calculated (with all other vortices "switched off"). When this loading is used as an input to an acoustic code such as WOPWOP, and the BVI sound pressure levels (determined from the acoustic signals) mapped on an observer plane, the resulting BVI noise (intensity and directionality) can be attributed to a single BVI event. By comparing results for each of the events (corresponding to specific vortices), and also for the entire wake, it is possible to determine the acoustically dominant events and their contributions to the total radiated BVI acoustic field. Such information could, in principle, be exploited to develop specific schemes that target elimination of the most detrimental interactions, or ensure that BVI alleviation schemes are "optimal" by not inadvertently strengthening some of the secondary events. Implementation results provided in the paper demonstrate the effectiveness as well as the accuracy of the decomposition procedure. It is further demonstrated that the impulsive loads, acoustic pressure, and BVI noise could be predicted without loss of accuracy by considering only portions of tip vortices generating close, near-parallel interactions in the 1st and 4th quadrants (instead of entire tip vortices comprising the rotor wake).

Acknowledgments

This research was supported by the US Army Research Office under the MURI Program entitled "Innovative Technologies for Actively Controlled Jet Smooth Quiet Rotorcraft" with Dr. Tom Doligalski as Technical Monitor.

References

1 Yu, Y. H., "Rotor Blade-Vortex Interaction Noise: Generating Mechanisms and its Control Concepts," *Proc. of the American Helicopter Society 2nd International Aeromechanics Specialists' Conference*, Bridgeport, Connecticut, Oct. 11-13, 1995.

2 Bagai, A., and Leishman, J. G., "Rotor Free-Wake Modeling using a Pseudo-Implicit Technique - Including Comparisons with Experimental Data," *Journal of the American Helicopter Society*, Vol. 40, No. 3, pp. 29-41, July 1995.

3 Tauszig, L., "Numerical Detection and Characterization of Blade-Vortex Interactions Using a Free Wake Analysis," MS Thesis, Department of Aerospace Engineering, The Pennsylvania State University, 1998.

4 Tauszig, L., and Gandhi, F., "Numerical Detection of Blade-Vortex Interactions Using a Free-Wake Analysis – A Comparison of Various Approaches," *Proc. of the 24th European Rotorcraft Forum*, Marseilles, France, Sept. 15-17, 1998.

5 Gandhi, F., and Tauszig, L., "A Critical Evaluation of Various Approaches for the Numerical Detection of Helicopter Blade-Vortex Interactions," *Journal of the American Helicopter Society*, Vol. 45, No. 3, July 2000, pp. 179-190.

6 Brooks, T. F., Booth, E. R., Boyd, D. D., Splettstoesser, W. R., Schultz, K. J., Kube, R., Niesl, G. H., and Sterby, O., "Analysis of a Higher Harmonic Control Test to Reduce Blade-Vortex Interaction Noise," *Journal of Aircraft*, Vol. 31, No. 6, Nov.-Dec. 1994, pp. 1341-1349.

7 Brooks, T. F., Boyd, D. D., Burley, C. L., and Jolly, J. R., "Aeroacoustic Codes for Rotor Harmonic and BVI Noise - CAMRAD.Mod1/HIRES," *Journal of the American Helicopter Society*, Vol. 45, No. 2, April 2000, pp. 63-79.

8 Brentner, K. S., "Prediction of Helicopter Rotor Discrete Frequency Noise - A Computer Program Incorporating realistic Blade Motions and Advanced Acoustic Formulation," NASA TM 87721, 1986.

9 Hoad, D. R., "Helicopter Model Scale Results of Blade-Vortex Interaction Impulsive Noise as Affected by Tip Modification," *Proc. of the 36th Annual Forum of the American Helicopter Society*, Washington DC, May 1980.

10 Martin, R. M., Elliott, J. W., and Hoad, D. R., "Experimental and Analytical Predictions of Rotor Blade Vortex Interaction," *Journal of the American Helicopter Society*, Vol. 31, No. 4, pp. 12 - 20, Oct. 1986.

11 Splettstoesser, W. R., Kube, R., Wagner, W., Seelhorst, U., Boutier, A., Micheli, F., Mercker, E., and Pengel, K., "Key Results from a Higher Harmonic Control Aeroacoustic Rotor Test (HART)," *Journal of the American Helicopter Society*, Vol. 42, No. 1, pp. 58-78, Jan. 1997.

12 Schmitz, F., and Sim, B. W., "Radiation and Directionality Characteristics of Advancing Side Blade-Vortex Interaction (BVI) Noise," *6th AIAA/CEAS Aeroacoustics Conference*, Lahaina, Hawaii, June 12-14, 2000.

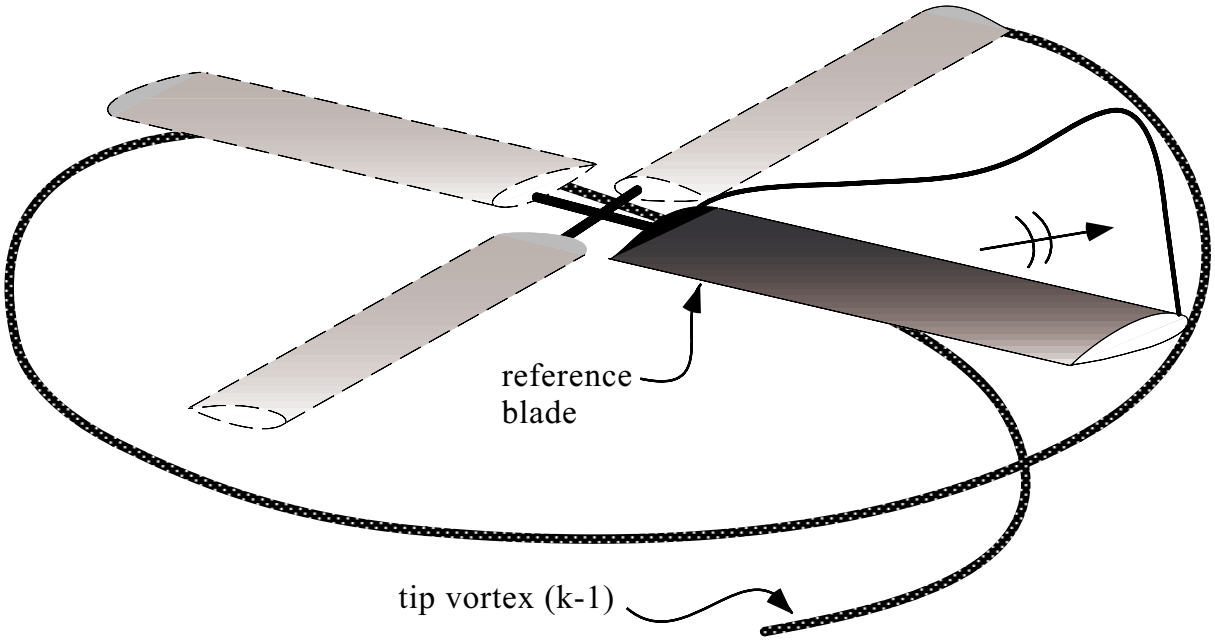

Figure 1: The loading due to one tip vortex on a reference blade is calculated. The corresponding acoustic pressures are then computed by WOPWOP.

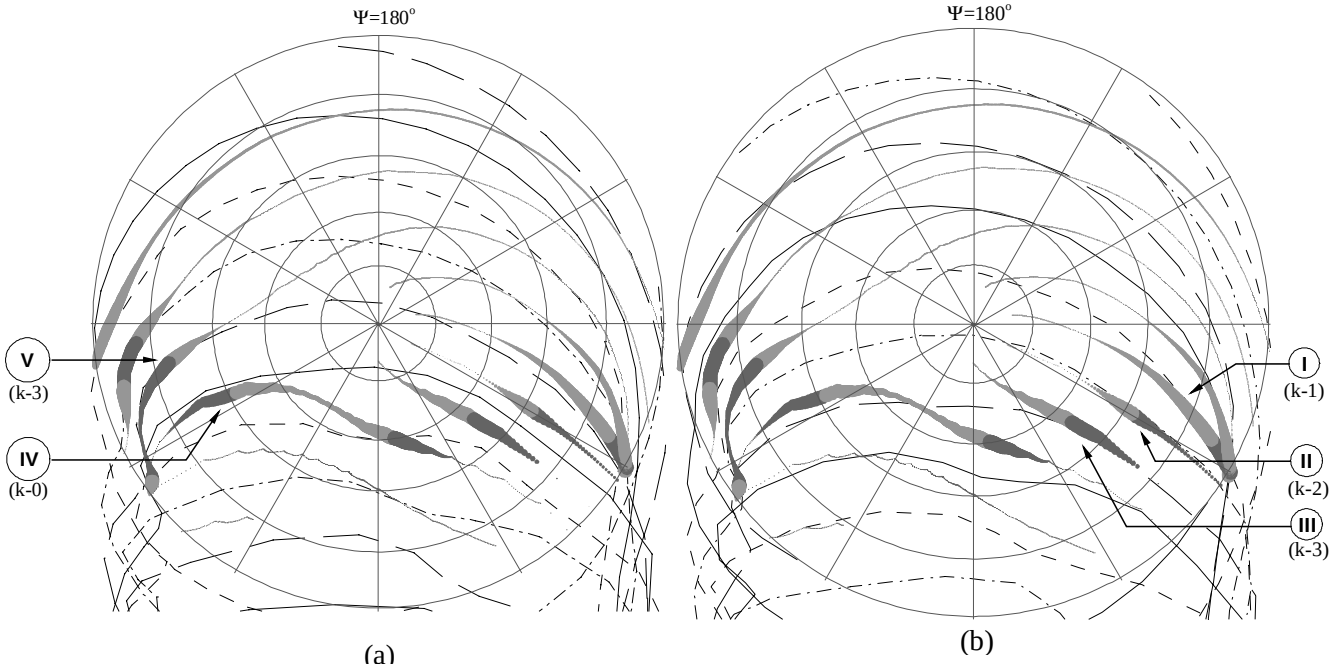

Figure 2: Location of parallel BVI on advancing and retreating sides (1st and 4th quadrants). (a) Location of vortices when reference blade is at ψ=285°. (b) Location of vortices when reference blade is at ψ=60°.

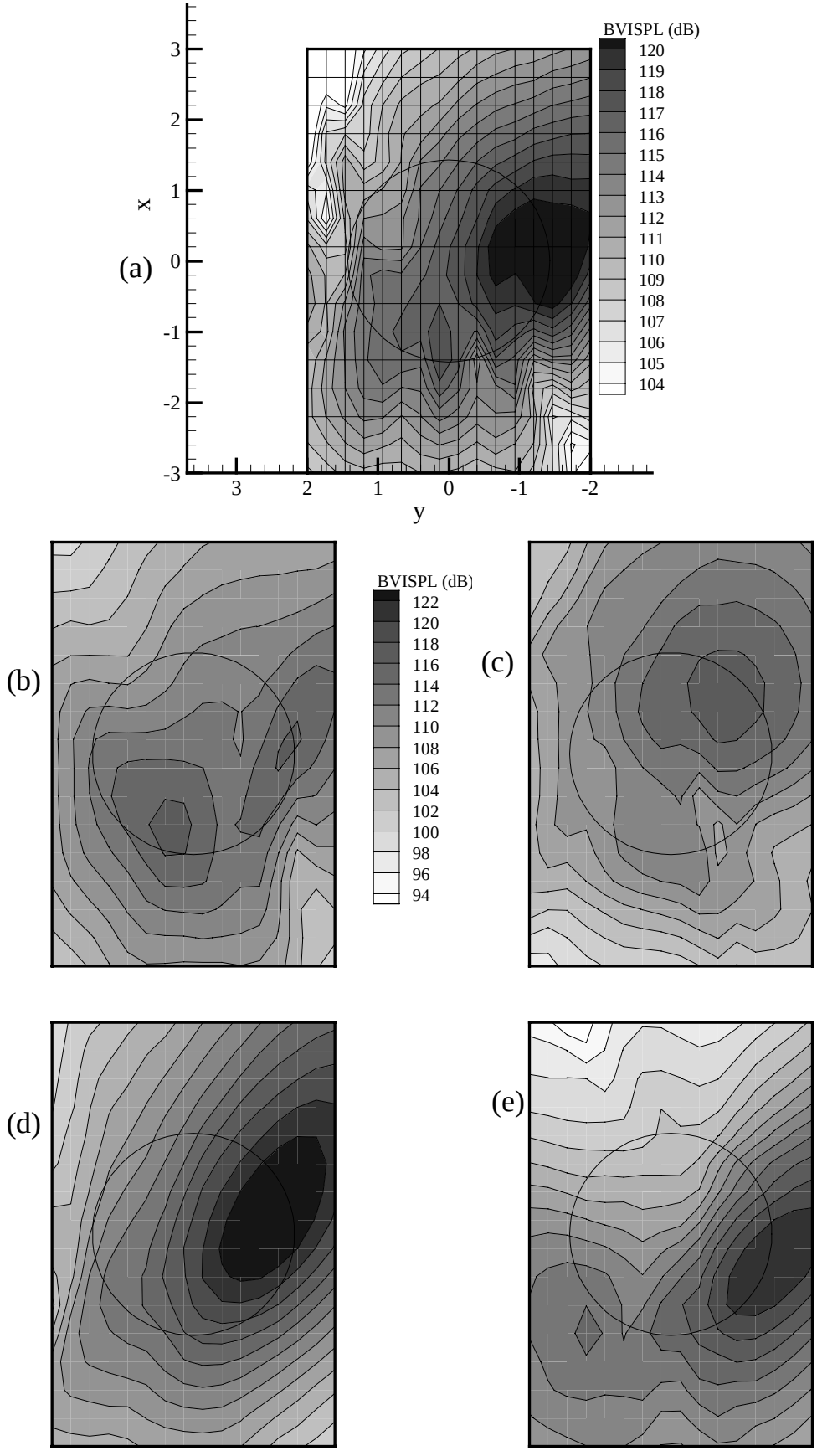

Figure 3: Noise (BVISPL) generated by the loading from (a) all the tip vortices (entire wake) (b) tip vortex from reference blade, k-0, (c) tip vortex from previous blade, k-1, (d) tip vortex from opposite blade, k-2, and (e) tip vortex from k-3.

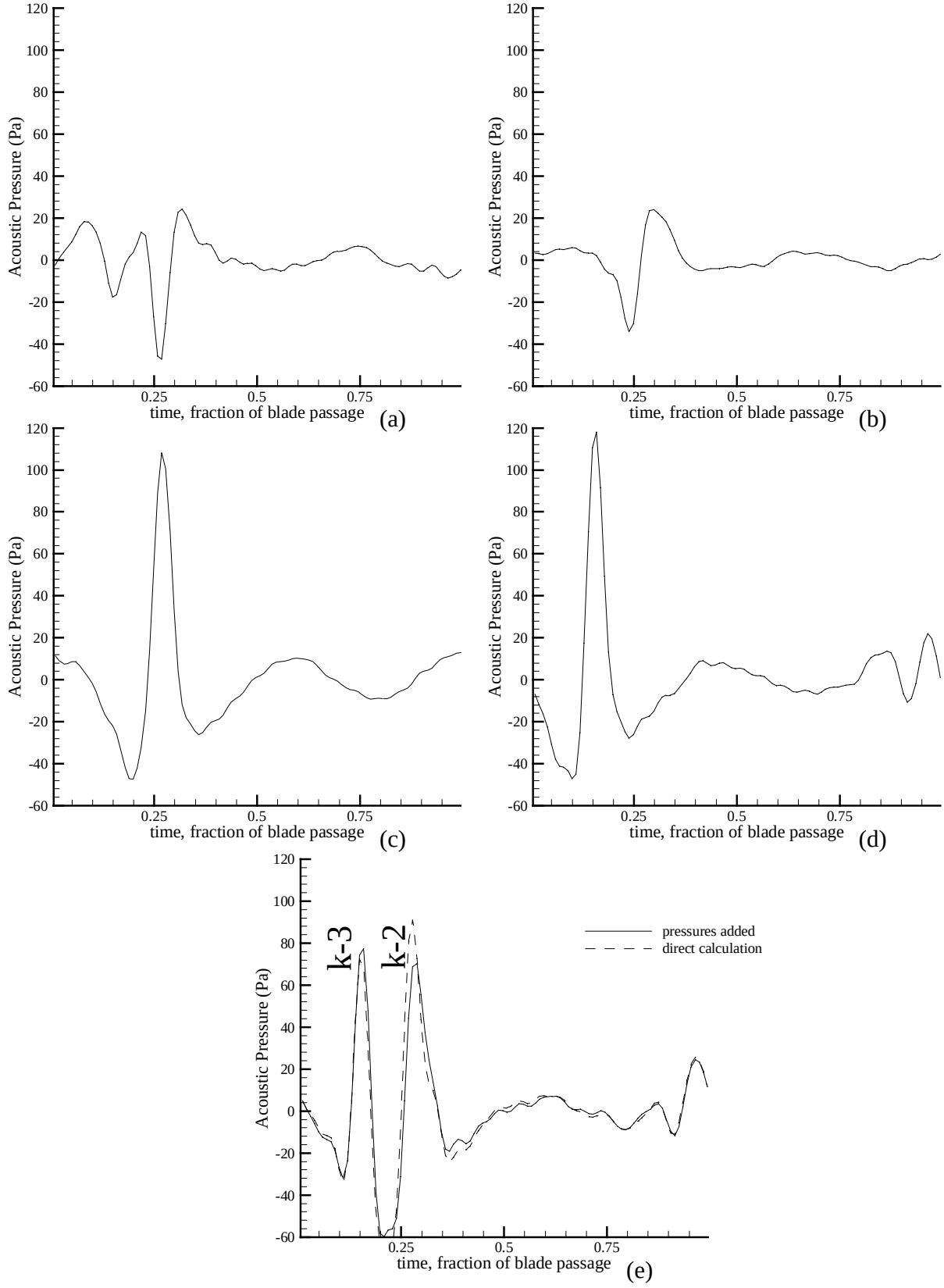

Figure 4: Comparison of BVI acoustic pressure time history at observer location (-0.2m, -1.5m) due to (a) vortex k-0, (b) vortex k-1, (c) vortex k-2, (d) vortex k-3 and (e) all the vortices (entire wake).

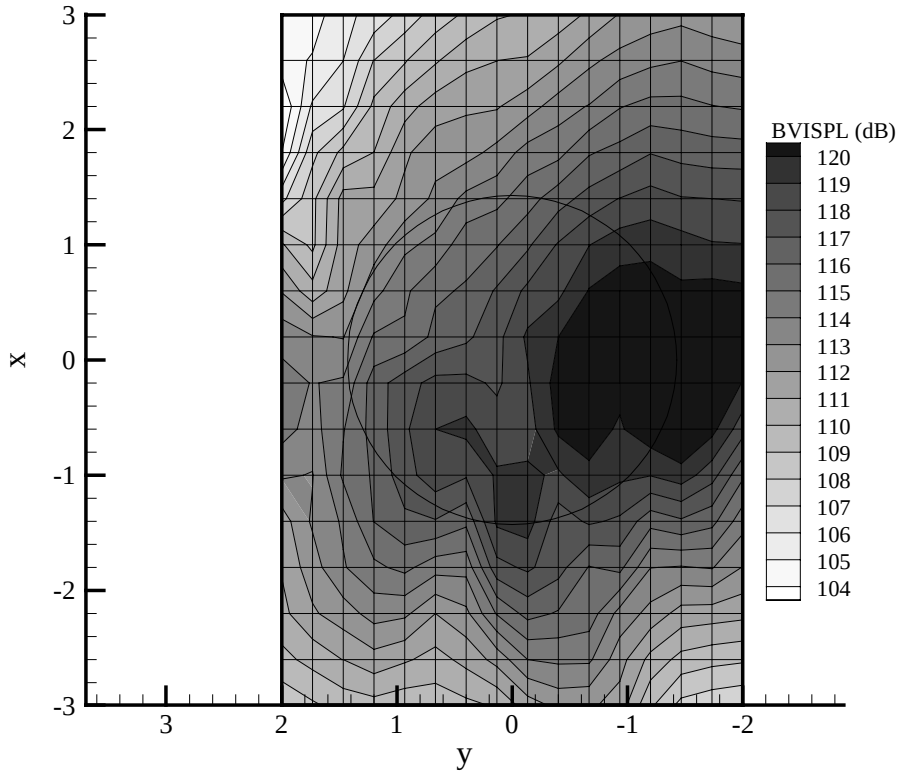

Figure 5: BVI Sound Pressure Levels reconstructed from the different tip vortices.

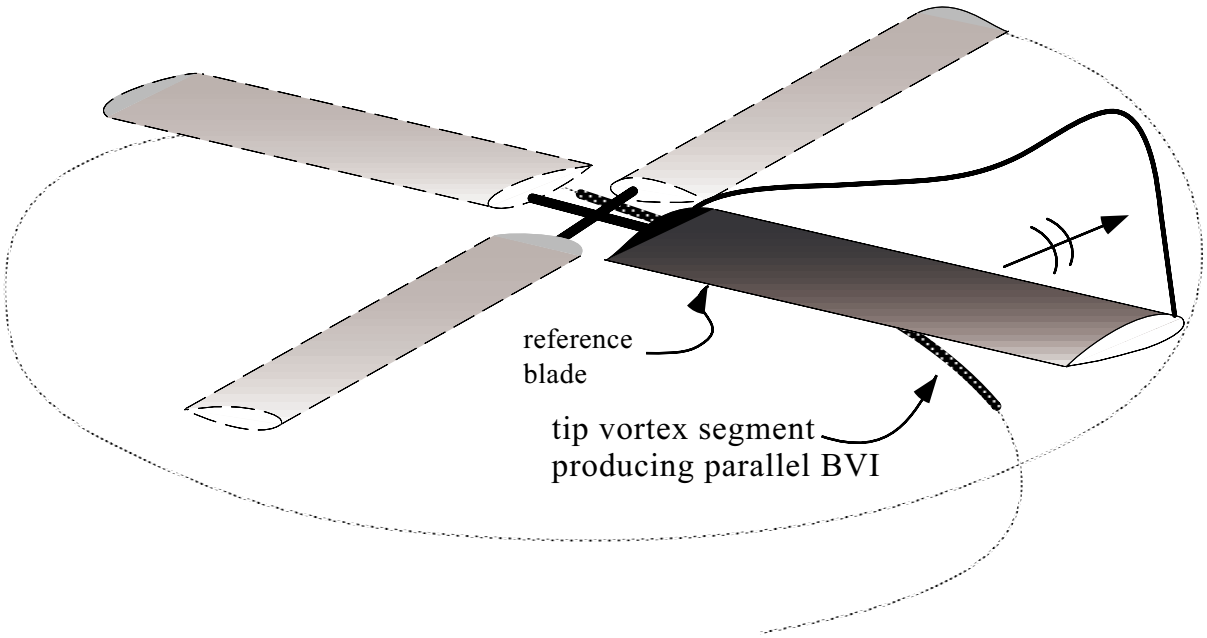

Figure 6: The loading due to only that portion of the tip vortex that produces BVIs in the 1st and 4th quadrant is calculated. The corresponding acoustic pressures are then computed by WOPWOP.

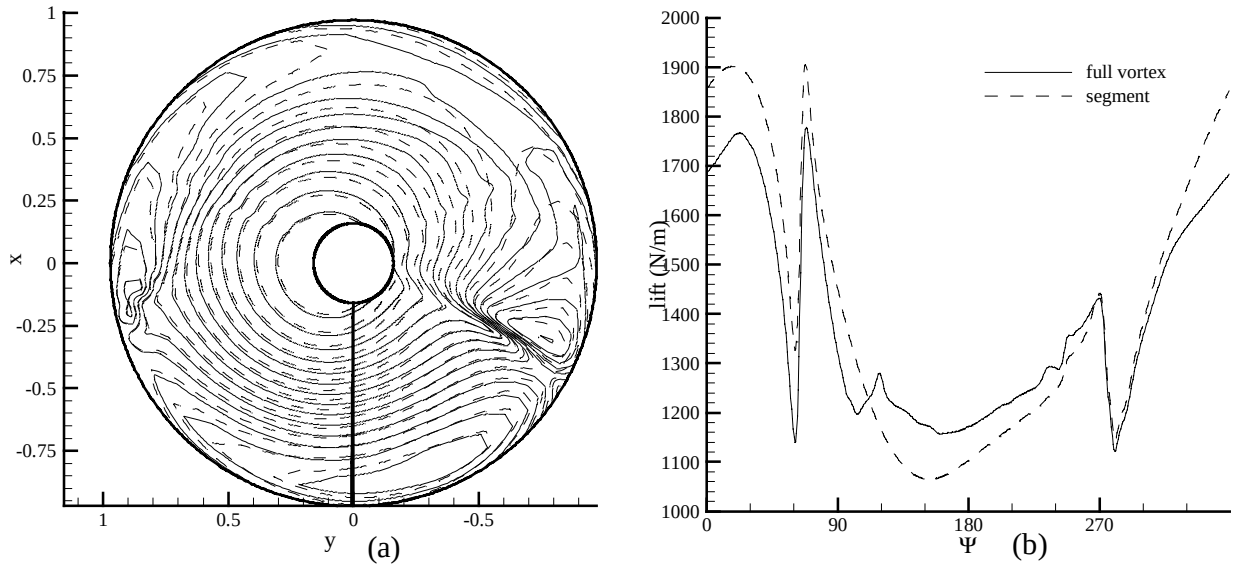

Figure 7: Comparison of the lift generated by the full tip vortex (k-2) and by the two segments of (k-2) producing BVIs in the 1st and 4th quadrants, (a) for the entire disk and (b) at the 80%R radial location.

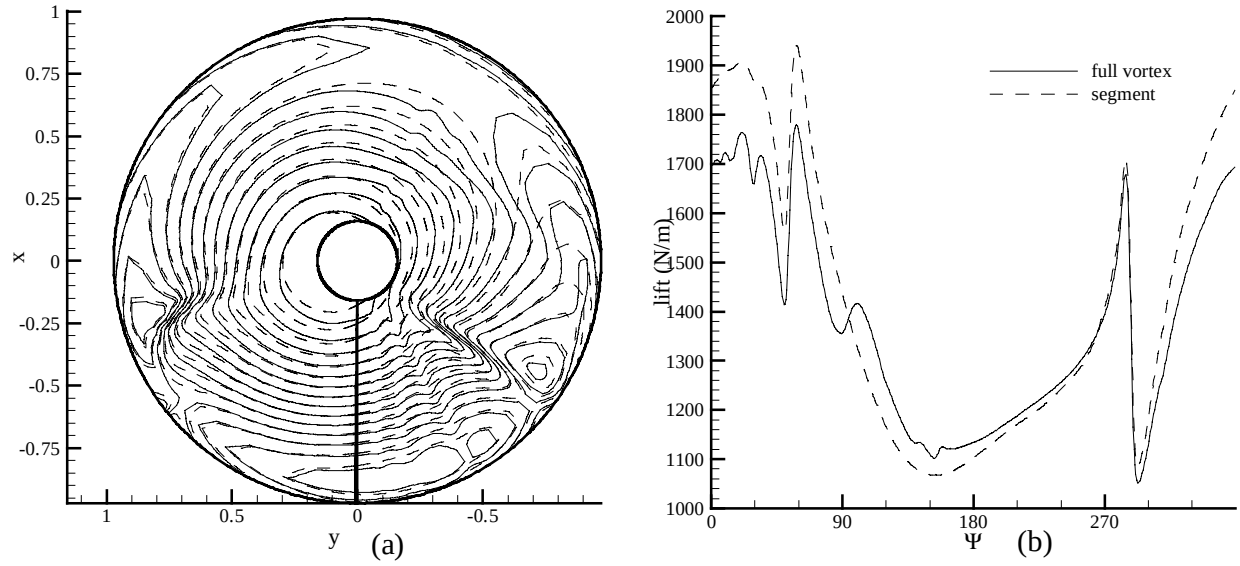

Figure 8: Comparison of the lift generated by the full tip vortex (k-3) and by the two segments of (k-3) producing BVIs in the 1st and 4th quadrants, (a) for the entire disk and (b) at the 80%R radial location.

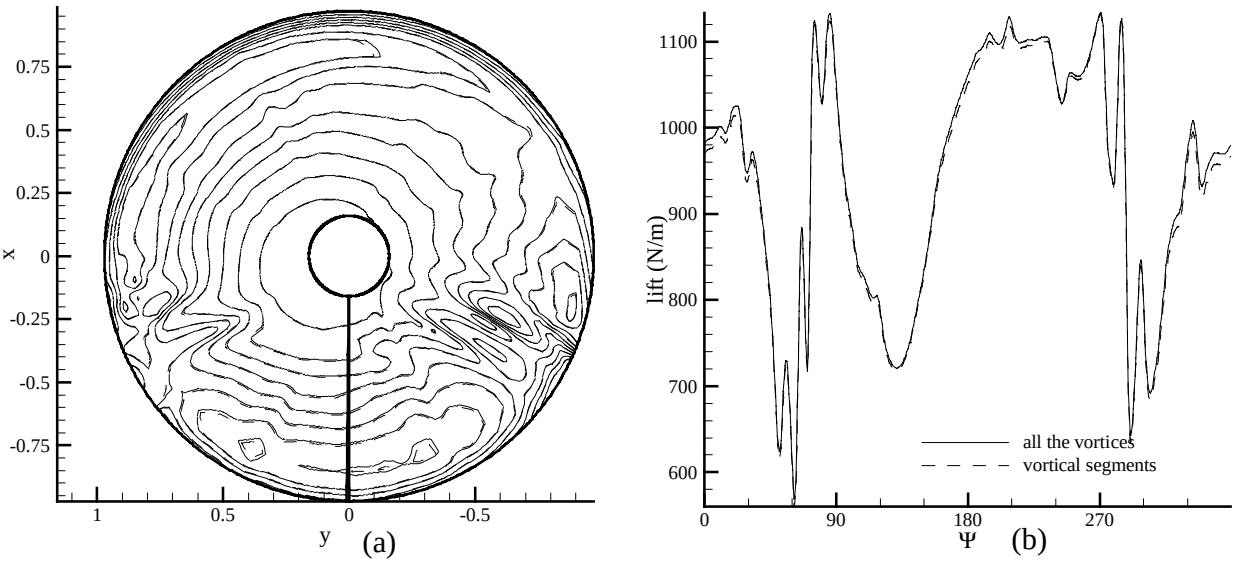

Figure 9: Comparison of the lift generated by all the tip vortices (entire wake) and by the 8 vortical segments producing BVIs in the 1st and 4th quadrants, (a) for the entire disk and (b) at the 80%R radial location.

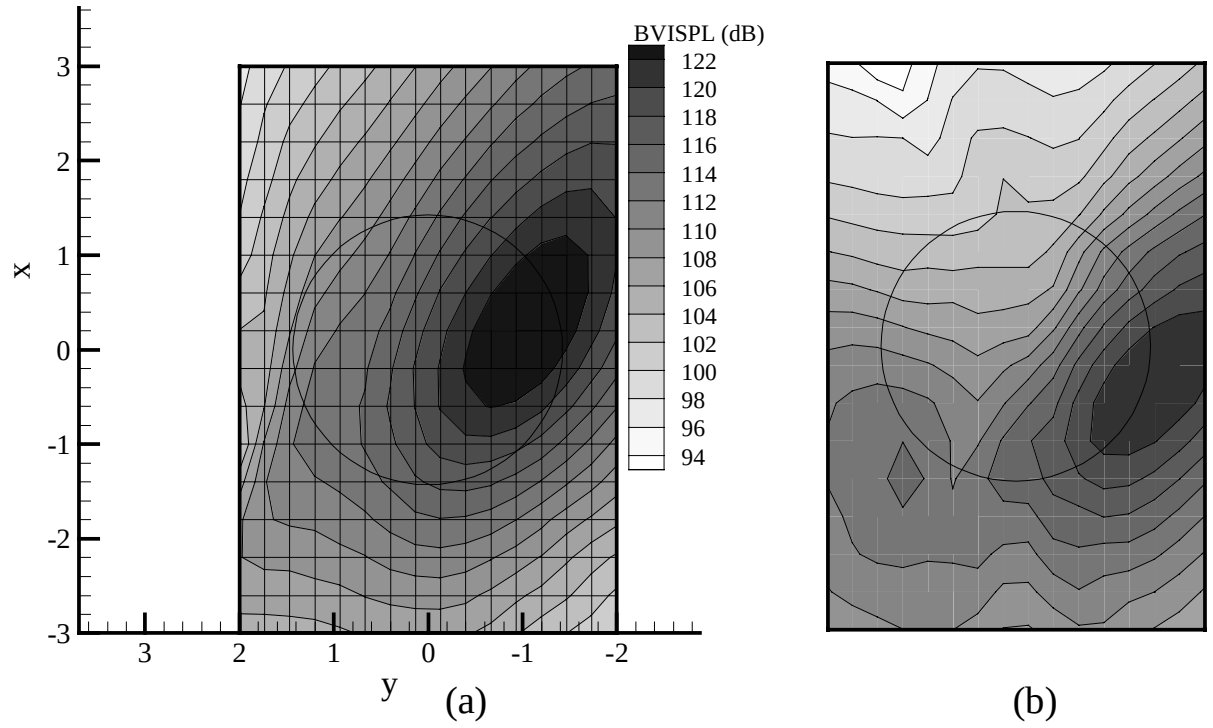

Figure 10: Noise generated (BVISPL) by (a) the (k-2) segments and (b) the (k-3) segments, in the 1st and 4th quadrants.

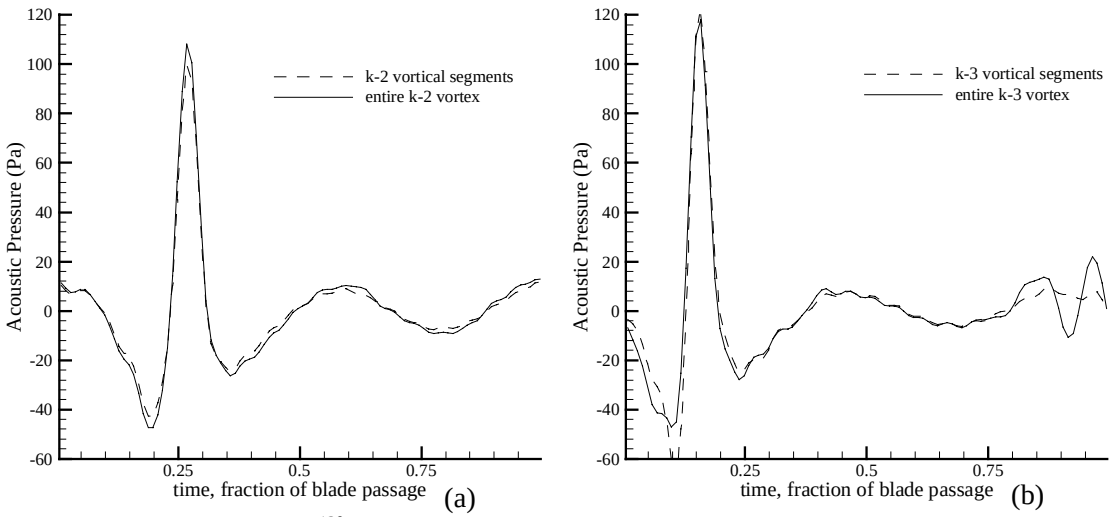

Figure 11: Comparison of BVI Sound Pressure Level from (a) k-2 segments, and (b) k-3 segments